The slow Ca^{2+}-activated K^+ current, I_{AHP}, in the rat sympathetic neurone

O. Sacchi, M. L. Rossi and R. Canella

Istituto di Fisiologia Generale dell' Università, Via Borsari 46, 44100 Ferrara, Italy

1. Adult and intact sympathetic neurones of the rat superior cervical ganglion maintained *in vitro* at 37 °C were analysed using the two-electrode voltage-clamp technique in order to investigate the slow component of the Ca^{2+}-dependent K^+ current, I_{AHP}.

2. The relationship between the after-hyperpolarization (AHP) conductance, g_{AHP}, and estimated Ca^{2+} influx resulting from short-duration calcium currents evoked at various voltages proved to be linear over a wide range of injected Ca^{2+} charge. An inflow of about $1{\cdot}7 \times 10^7$ Ca^{2+} ions was required before significant activation of g_{AHP} occurred. After priming, the g_{AHP} sensitivity was about 0·3 nS pC^{-1} of Ca^{2+} inward charge.

3. I_{AHP} was repeatedly measured at different membrane potentials; its amplitude decreased linearly with membrane hyperpolarization and was mostly abolished close to the K^+ reversal potential, E_K (−93 mV). The monoexponential decay rate of I_{AHP} was a linear function of total Ca^{2+} entry and was not significantly altered by membrane potential in the −40 to −80 mV range.

4. Voltage-clamp tracings of I_{AHP} could be modelled as a difference between two exponentials with $\tau_{on} \approx 5$ ms and $\tau_{off} = 50$–250 ms.

5. Sympathetic neurones discharged only once at the onset of a long-lasting depolarizing step. If I_{AHP} was selectively blocked by apamin or D-tubocurarine treatments, accommodation was abolished and an unusual repetitive firing appeared.

6. Summation of I_{AHP} was demonstrated under voltage-clamp conditions when the depolarizing steps were repeated sufficiently close to one another. Under current-clamp conditions the threshold depolarizing charge for action potential discharge significantly increased with progressive pulse numbers in the train, suggesting that an opposing conductance was accumulating with repetitive firing. This frequency-dependent spike firing ability was eliminated by pharmacological inhibition of the slow I_{AHP}.

7. The I_{AHP} was significantly activated by a single action potential; it was turned on cumulatively by Ca^{2+} load during successive action potential discharge and acted to further limit cell excitability.

Influx of calcium via voltage-dependent channels leads to activation of a heterogeneous class of ion channels including two types of K^+ channel, the so-called BK (Marty, 1981; Smart, 1987; Latorre, Oberhauser, Labarca & Alvarez, 1989) and SK channels (Blatz & Magleby, 1986; Lang & Ritchie, 1987; Lancaster, Nicoll & Perkel, 1991; Leinders & Vijverberg, 1992; Artalejo, García & Neher, 1993), which are of interest for neuronal functioning. They all decrease excitability by increasing membrane conductance and hyperpolarizing the membrane potential, but differ markedly in their temporal and functional characteristics. In many cells activation of BK channels contributes, in a variable mix with the other K^+ currents such as the K^+ delayed rectifier current, I_{KV}, and the fast transient K^+ current, I_A, to action potential repolarization, while the SK channels are suggested to underlie the current generating the spike after-hyperpolarization (AHP). The SK channels, with their high Ca^{2+} sensitivity and limited voltage dependence, control the spike response to long-duration current pulses on the one hand and on the other hand contribute to the background membrane conductance during rapid firing. The rat sympathetic neurone very effectively adapts to long-duration current pulses and is physiologically exposed to ongoing synaptic stimulation, of variable intensity and frequency, driving different firing patterns (Blackman, 1974; Polosa, Mannard & Laskey, 1979). Both aspects of neuronal behaviour have been analysed on adult intact rats sympathetic neurones, in which current-clamp experiments have only provided indirect evidence of the relationship between the AHP generating current and the transmembrane calcium movements (Kawai & Watanabe, 1986).

In the present report we first describe the relationship between Ca^{2+} load and I_{AHP} activation as obtained in voltage-clamp experiments. We then describe the conditions allowing I_{AHP} summation following Ca^{2+} injection. Finally, from these measurements we develop a quantitative, empirical description of the I_{AHP} and, taking advantage of a previous multi-conductance model of the rat sympathetic neurone (Belluzzi & Sacchi, 1991), we show how activation of the I_{AHP} influences the overall electrical activity of the cell.

METHODS

Experiments were performed on superior cervical ganglia isolated from young rats (100–130 g body wt) under urethane anaesthesia (1 g kg^{-1}; I.P. injection) and maintained *in vitro* at 37 °C. After surgery, the animals were killed with an overdose of anaesthetic. Ganglia were mounted on the stage of a compound microscope; intact and mature neurones were identified at a magnification of ×500 using Nomarski optics and impaled with two independent glass microelectrodes filled with neutralized 4 M potassium acetate and having resistances of 30–45 MΩ. The cells were current and/or voltage clamped using a custom-made two-electrode voltage-clamp amplifier as previously described (Belluzzi, Sacchi & Wanke, 1985). For recordings, ganglia were superfused with a medium (gassed with 95% O_2 and 5% CO_2, giving a pH of 7·3), of the following composition (mM): NaCl, 136; KCl, 5·6; $CaCl_2$, 5; $MgCl_2$, 1·2; NaH_2PO_4, 1·2; $NaHCO_3$, 14·3; glucose, 5·5. When the Ca^{2+}-dependent current components were isolated, the initial bathing medium was switched to a $H_2PO_4^-$- and HCO_3^--free medium whose composition was (mM): NaCl, 136; KCl, 5·6; $CaCl_2$, 5; $MgCl_2$, 1·2; Tris–HCl, 15; glucose, 5·5 (pH 7·3). Cadmium chloride (0·3–0·5 mM) was then included in the perfusing medium without osmotic compensation. The drugs used were apamin (Alomone Labs, Jerusalem) and D-tubocurarine chloride (Calbiochem, USA).

Data acquisition and pulsing were governed by an IBM 386 personal computer interfaced through an A/D converter (Labmaster/TL-1 interface; Axon Instruments, USA) operating pCLAMP software (Axon Instruments). Single currents were filtered at 5 kHz using an 8-pole Bessel filter, digitized at 1–5 kHz and stored on disk for further analysis. Trains of voltage-command signals were generated by a function generator and fed directly to the voltage-clamp amplifier. For current-clamp recordings the current amplifier was connected to an external stimulator, which allowed continuous stimulation through the current electrode at various frequencies. Brief current injections (2–3 ms) were employed to evoke action potentials. Long-lasting current tracings containing trains of voltage pulses and records under current-clamp conditions were filtered at 10 kHz (8-pole Bessel filter) and recorded continuously on a digital tape recorder (DTR1204, Biologic; DC to 10 kHz). Stored data were transferred to the computer through the A/D converter using the data acquisition software.

The five-conductance model of the somatic membrane of the mature rat sympathetic neurone, presented in a previous study (Belluzzi & Sacchi, 1991), was used to simulate the neurone behaviour under current-clamp conditions. Basically, five separate types of voltage-dependent ionic conductance have been individually isolated at 37 °C using a two-electrode voltage-clamp method, and kinetically characterized in the framework of the Hodgkin–Huxley scheme. The mathematical functions for the activation and inactivation (whenever present) gating mechanisms of each current over a wide voltage range are available in the paper indicated above (text eqns (7)–(11) for the sodium current, I_{Na}; eqns (13)–(16) for the calcium current, I_{Ca}; eqns (22)–(23) for the K^+ delayed rectifier, I_{KV}; eqns (24)–(27) for the fast transient K^+ current, I_A; eqns (29)–(32) for the Ca^{2+}-dependent K^+ current, $I_{K,Ca}$). We report here the values of the constants used in the present computations: $g_{Na,fast}$, 9·28 μS per neurone; $g_{Na,slow}$, 7·43 μS; P_{Ca}, $2{\cdot}09 \times 10^{-8}$ cm s^{-1}; g_{KV}, 0·44 μS; g_A, 2·30 μS; $g_{K,Ca,fast}$, 0·45 μS; $g_{K,Ca,slow}$, 0·62 μS; g_L, 0·08 μS; E_{Na}, +40·0 mV; E_L, −73·2 mV. E_K is expected to move from the −93·0 mV at rest because of K^+ accumulation in the perineuronal space during outward current flow (see Belluzzi & Sacchi, 1991; text eqn (18)). When, however, the actual electrical response of a neurone was compared to the predictions of the model, the values for membrane capacitance, C_m, and leak conductance, g_L, used in the simulation were chosen so as to yield the cell input resistance and time constant directly measured in that neurone.

RESULTS

I_{AHP} general properties

Step depolarization of a voltage-clamped rat sympathetic neurone activates a plethora of ionic currents so that when the membrane potential returns to the holding level (or beyond) a sequence of summated tail currents is revealed. These are dominated by a large outward tail current which decays in a few milliseconds leaving, for a few additional hundred milliseconds, a small slow component, as partially illustrated in Fig. 1*A* for a neurone held at −50 mV. Previous studies (Belluzzi & Sacchi, 1990; Belluzzi & Sacchi, 1991) have demonstrated that the fast large tail current corresponds to deactivation of the two major K^+ currents, the calcium-activated K^+ current $I_{K,Ca}$ and I_{KV} (I_A is inactivated by the holding voltage and I_{Na} is activated by depolarization but fully inactivates within 1 ms), while the long-lasting tail current corresponds to the I_{AHP}, as recognized for this and other cells (Hirst, Johnson & van Helden, 1985; Pennefather, Lancaster, Adams & Nicoll, 1985; Lancaster & Adams, 1986; Tanaka & Kuba, 1987; Morita & Katayama, 1989; Sah & McLachlan, 1991). Membrane repolarization efficiently contributes to the rapid closure of voltage-dependent channels since $I_{K,Ca}$ deactivates with a mean time constant of 1·1 ms at −50 mV and I_{KV} with a time constant of 5·2 ms (both becoming faster with increasing membrane negativity; Belluzzi & Sacchi, 1990) so that this process can be considered fully completed within 30 ms. In the present study I_{AHP} was thus measured 40 ms after the step-down from the depolarizing pulse to holding potential to avoid interference by other K^+ currents. Application of 0·5 mM Cd^{2+} abolished both the slow small tail and most of the fast large tail, of which only the Ca^{2+}-independent I_{KV} fraction survives (Fig. 1*B*).

The depolarizing steps were followed by a distinct I_{AHP}, provided that the membrane potential during the voltage

pulse was sufficiently positive, to a level that evoked Ca^{2+} entry ($\geqslant -30$ mV). Figure 1 shows that I_{AHP} was Ca^{2+} dependent and increased in amplitude with an increase in step duration and, therefore, Ca^{2+} load. I_{AHP} currents were repetitively obtained with test pulses of different amplitude and various durations. Since it was not practical to measure I_{AHP} and the generating I_{Ca} in each cell and for each pulse, the I_{Ca} and associated tail current corresponding to the individual depolarizing steps were reconstructed, taking advantage of a previous quantitative model for the calcium current developed for this neurone (Belluzzi & Sacchi, 1989); the value for the charge carried by the Ca^{2+} ions (Q_{Ca}) derived from the integral of I_{Ca} under the different conditions was considered to be a reliable measure of calcium influx. Noting that I_{AHP} is measured at a known holding potential, that the I_{AHP} null potential is about -93 mV (see below) and that the AHP channel is apparently non-rectifying over the -40 to -90 mV voltage range (Lang & Ritchie, 1987; Lancaster *et al.* 1991; Leinders & Vijverberg, 1992), the relationship between Ca^{2+} load and activated g_{AHP} was obtained (Fig. 2*A*). I_{AHP} remained undetectable for a Ca^{2+} influx smaller than the one induced by a single 1 ms pulse to -10 mV. Larger Q_{Ca} values produced larger values of g_{AHP}, the increase being linear and apparently non-saturating over the range of Q_{Ca} shown. Inspection of the g_{AHP} *versus* Q_{Ca} plot makes it apparent that influx of Ca^{2+} is required before I_{AHP} is activated and thereafter, similarly to the $I_{K,Ca}$ behaviour (Belluzzi & Sacchi, 1990), I_{AHP} develops abruptly. The mean I_{Ca} current integral just-threshold for activation of measurable I_{AHP} was 7 pC; allowing for priming, a measurement of the activation of g_{AHP} by calcium influx is the ratio of peak g_{AHP} to Q_{Ca}; the mean ratio of g_{AHP} to the inward charge carried by Ca^{2+} ions was 0·3 nS pC^{-1}. It is evident from Figs 1*A* and 2*B* that I_{AHP} was unambiguously activated by voltage pulses as short as 1 ms. This observation may be related to the functional role sustained by g_{AHP} during normal spike activity. In previous computations of rat sympathetic neurones we suggested that the time during which the calcium channels are opened by the voltage modifications associated with action potential development is 1 ms and that during this time 11 pC of Ca^{2+} are injected into the neurone, this figure becoming slightly smaller with an increase in holding potential (Belluzzi & Sacchi, 1989). In six cells where short pulses were applied in a different mix of amplitude and duration but with the common result of injecting approximately 11 pC of Ca^{2+} into the neurone, the mean

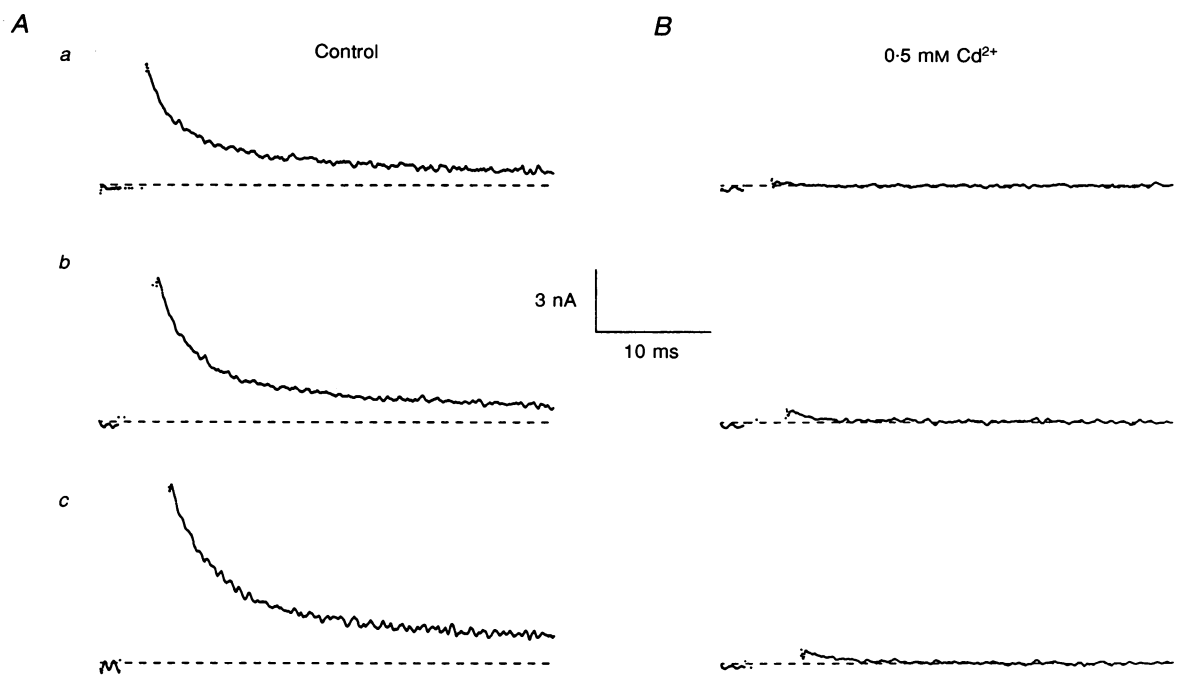

Figure 1. Tail currents following voltage-clamp pulses of varying duration

Tail currents following a voltage-clamp pulse to +10 mV of 1 (*a*), 2 (*b*) and 4 ms (*c*) duration observed at the holding potential of -50 mV in a rat sympathetic neurone maintained in control solution (*A*) or after bath application of 0·5 mM Cd^{2+} (*B*). The outward currents evoked by the depolarizing steps (off scale) were of 33·3, 62·8 and 86·3 nA peak amplitude (*a–c*) in *A* and of 15·0, 19·9 and 22·2 nA in the presence of Cd^{2+}. The recordings in *A* show the rapid turn-off of the delayed K^+ currents $I_{K,Ca}$ and I_{KV} and their smooth prolongation into the I_{AHP} current component. In *B*, the Ca^{2+}-dependent current fraction is cancelled and only the I_{KV} tail currents survive. Dashed lines indicate zero current level.

measured g_{AHP} was 8·7 ± 2·1 nS, in agreement with the result suggested by the calibration curve in Fig. 2*A* relating g_{AHP} to the amount of injected calcium. The AHP amplitude, on the other hand, can provide an indirect measure of change in conductance if the cell resistance and the I_{AHP} equilibrium potential are known (Ginsborg, 1973). In twelve cells exhibiting a mean input resistance of 35 MΩ the AHP amplitude at 30 ms from the spike peak was 8·7 ± 2·1 mV (similar estimates by McAfee & Yarowsky, 1979) which would correspond again to a conductance increase of about 8·9 nS. The appearance of the late I_{AHP} in the voltage-clamp experiments and the AHP elicited by a single action potential are thus different aspects of the same phenomenon. These observations therefore agree, and indicate that the g_{AHP} operated by a single action potential was 8–10 nS.

When longer and wider depolarizing pulses were used, I_{AHP} became larger and decayed more slowly. The I_{AHP} tail was usually well fitted by a single exponential; total calcium entry thus affected not only the resultant I_{AHP} amplitude but also its decay rate. This is shown in Fig. 2*C*, in which g_{AHP} was evoked and measured in experiments similar to those illustrated in Fig. 2*A*. The straight line would roughly indicate that the I_{AHP} decay rate increases by approximately 10 ms per nanosiemens of activated g_{AHP}.

The voltage dependence of the I_{AHP} time course was investigated next. The time constant of I_{AHP} decay (τ_{AHP}), in contrast to the clear-cut voltage-dependent behaviour of $I_{K,Ca}$, remained constant in the range of membrane potential from −40 to −70 mV. In the six cells studied, no definite trend for τ_{AHP} could be detected; thus the kinetics of I_{AHP} showed little or no voltage dependence.

The effect of returning to different levels of membrane potential immediately after the depolarizing step activating the I_{AHP} was also examined. Only a limited voltage range could be tested because, at potentials positive to −40 mV, large and persistent voltage-dependent K^+ currents were

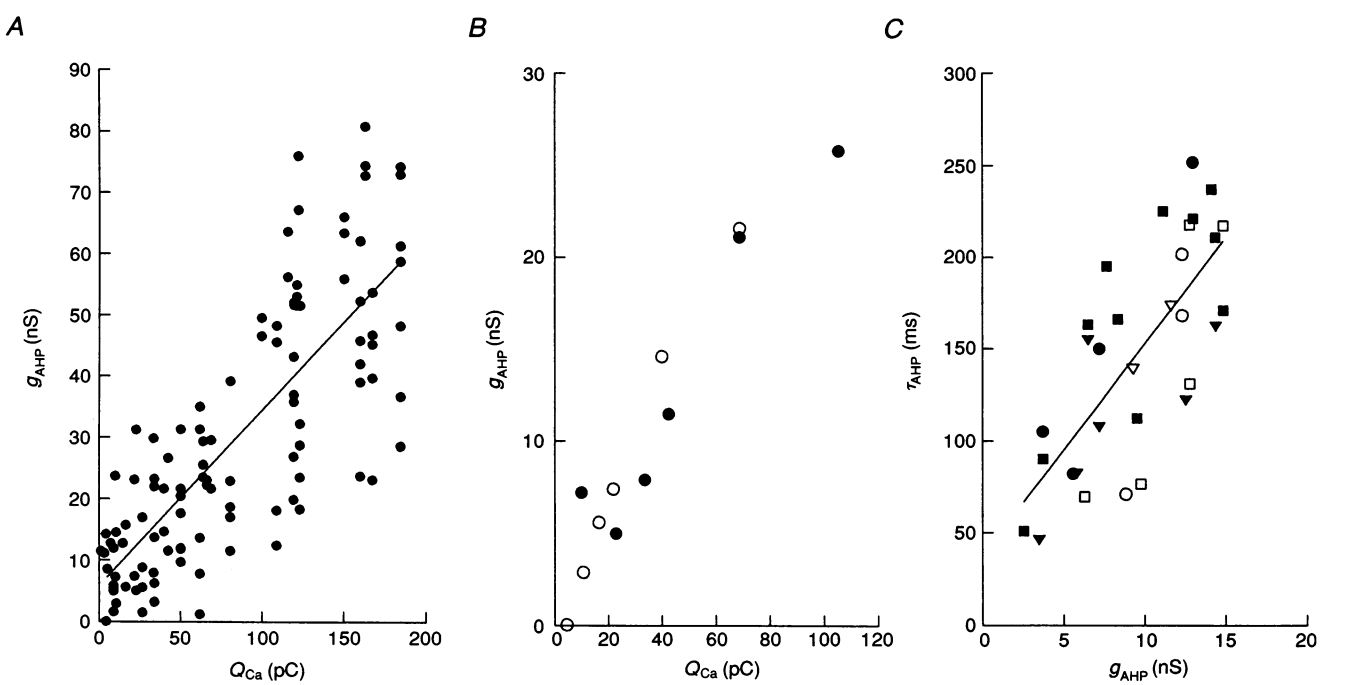

Figure 2. Ca^{2+} dependence and time course of activated g_{AHP}

A shows the relationship between Ca^{2+} load and activated g_{AHP}. Data are from 14 different neurones following voltage-clamp pulses in the −20 to +20 mV voltage range (1–80 ms duration); the evoked I_{AHP} was measured at −50 mV, 40 ms following step-down from the depolarizing pulse to the holding potential. The amount of injected Ca^{2+} was obtained from the integral of the calcium currents reconstructed for each depolarizing step in an ideal sympathetic neurone according to the I_{Ca} kinetics and Ca^{2+} permeability described in a previous study (Belluzzi & Sacchi, 1989). The regression line through pooled data points is drawn according to the equation $y = 0{\cdot}3x + 5{\cdot}8$ with a correlation coefficient $r = 0{\cdot}795$ (Student's t test for the significance of the regression coefficient gives $t = b/s_b = 10{\cdot}8$ with $P < 0{\cdot}001$). *B*, g_{AHP} activation in 2 different neurones plotted against Ca^{2+} inflow during repeated voltage-clamp pulses to −10 mV (○) or 0 mV (●) of 1, 2, 3, 4, 8 and 16 ms duration. The holding potential was −50 mV. *C*, the relationship between activated g_{AHP} and the decay time constant of the generated I_{AHP}. The conductance range considered was limited to the g_{AHP} values presumably activated by action potential discharge. The regression line through data points is drawn according to the equation $y = 11{\cdot}53x + 37{\cdot}38$.

readily activated and at rather negative potentials the I_{AHP} became too small to measure. Membrane currents elicited by repetitively applied −50 to 0 mV pulses of 4 ms duration, and observed in the −40 to −90 mV voltage range, are illustrated in Fig. 3*A–C*. When the holding potential was altered, the amplitude of the tail current changed in relation to the corresponding leakage current which, in the absence of I_{AHP}, was the only current present at membrane potentials negative to −40 mV. It can be seen that the I_{AHP} became smaller with increasing membrane negativity. The pure Ca^{2+}-dependent nature of this current was further studied in experiments in which the protocol partially shown in Fig. 3*A–C* was repeated in the presence of 0·5 mM Cd^{2+}. The peak amplitudes of the slow difference currents elicited in this way are plotted against return membrane potential, as illustrated for two different neurones in Fig. 3*D*. It is evident that in both cells the I_{AHP} null potential was about −90 mV, close to the Nernstian K^+ equilibrium potential for a sympathetic neurone (−93 mV), a finding which implies that the conductance change underlying the I_{AHP} was an increase in K^+ conductance.

I_{AHP} summation

Since relevant characteristics of neuronal behaviour, such as repetitive firing and adaptation, seem to depend largely upon the summative properties of the AHP, the build-up of g_{AHP} was analysed under voltage-clamp conditions during trains of depolarizing pulses of different amplitude and duration (applied at variable rates). Figure 4*A* shows a neurone which was repetitively depolarized to −20 mV for 3 ms at 20 Hz. Accumulation of I_{AHP} occurred and, if this pulse sequence was used, it became saturated after the tenth pulse. The change in I_{AHP} relating to the second

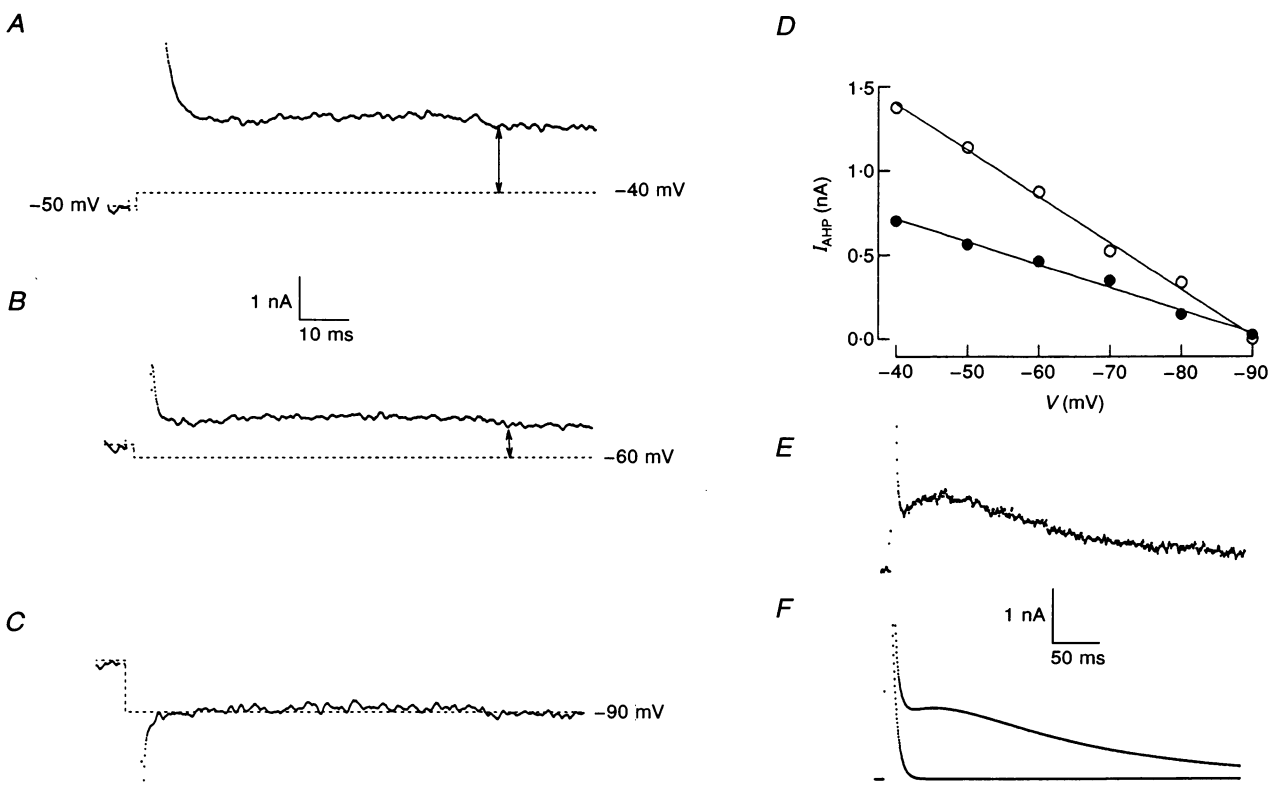

Figure 3. I_{AHP} properties and null potential in the sympathetic neurone

A–C, voltage-clamp tracings from a neurone repeatedly pulsed to 0 mV for 4 ms and then repolarized in 10 mV steps in the −40 to −90 mV membrane voltage range. The tail currents recorded at −40 (*A*), −60 (*B*) and −90 mV (*C*), together with the corresponding leakage currents (dashed lines), are illustrated. Arrows indicate the I_{AHP} amplitude measured at the different holding levels. Holding potential was −50 mV. The same procedure was then repeated in the presence of 0·5 mM Cd^{2+}. The peak amplitudes of the difference currents thus obtained in the presence and absence of transmembrane Ca^{2+} movements are plotted against voltage to construct the *I–V* relationship for the almost pure I_{AHP} shown in *D* for 2 different neurones. The null potential for the I_{AHP} is close to −90 mV. *E*, tail currents observed in a sympathetic neurone at the holding potential of −50 mV following a voltage pulse to 0 mV of 5 ms duration. *F*, computed tracings in response to the same voltage step used in *E* calculated according to the neurone model properties (with $g_{AHP} = 40$ nS, $\tau_1 = 150$ ms, $\tau_2 = 45$ ms in text eqn (1)). Simulations are repeated in the presence or in the absence of the Ca^{2+}-dependent current components.

pulse was only a fraction of the first one; a further slight decrease occurred for the following pulse, until an equilibrium was gained when the new I_{AHP} contribution corresponded to the amount decayed during the preceding time interval. The long-lasting train was interrupted after the first or the fourth pulse to show the I_{AHP} decay time course. According to Fig. 2*C*, with an increase in Ca^{2+} load the decay time constant increased from 115 ms in the first tracing to 210 and 496 ms in the successive records. The same neurone was repetitively activated under current-clamp conditions (Fig. 4*B*) by a train of suprathreshold short current pulses applied through the current electrode at the same rate as in *A*. The fast negative deflections of membrane potential immediately after each spike were due to activation of $I_{K,Ca}$ and I_{KV}, while the much slower AHPs were caused by the I_{AHP} development. The membrane potential preceding the next spike became more hyperpolarized until a steady state was reached. The AHP growth, in fact, rapidly became saturated as no further increase in membrane negativity occurred after the tenth spike, a phenomenon which strictly parallels the one observed under voltage-clamp conditions.

In further trials, different modes of I_{AHP} summation were tested. In Fig. 4*C* pulses of increasing amplitude (−50 to −20, −50 to −10 and −50 to 0 mV) were repetitively applied to the same neurone at a constant rate (20 Hz). The

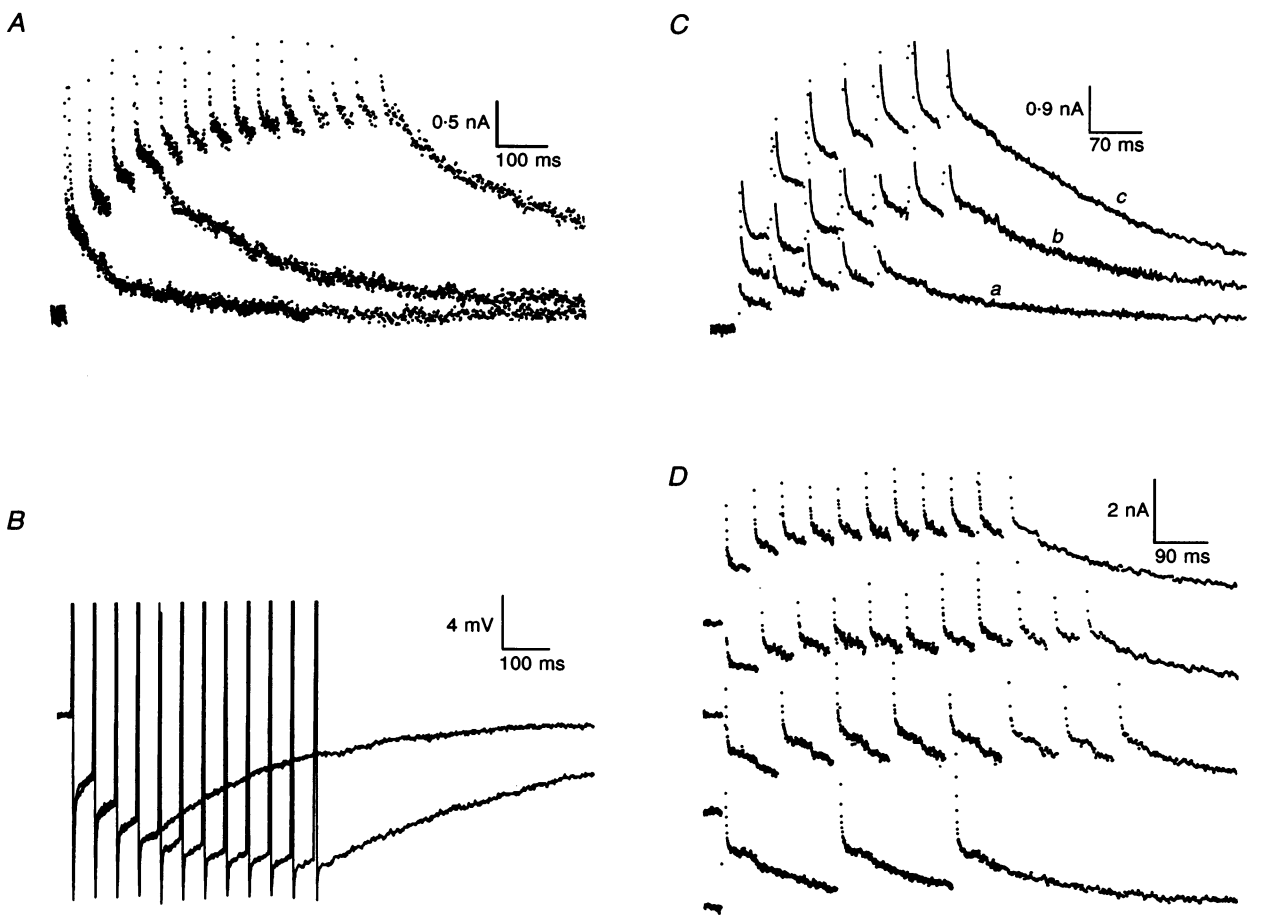

Figure 4. Summation of I_{AHP} in rat sympathetic neurone

A, a train of 14 constant voltage pulses of 3 ms duration from the holding potential of −50 mV to −20 mV applied at 20 Hz. The train is interrupted after the first and fourth steps in the series to demonstrate the increase in the I_{AHP} decay time constant (115, 210 and 496 ms, respectively) with increased g_{AHP} activation. *B*, recordings under two-electrode current-clamp conditions from the same neurone shown in *A* illustrate the progressive summation of AHP during a train of 11 action potentials (off scale) elicited at 20 Hz by short current pulses applied to the cell through the current electrode. The stimulation was discontinued after the fourth spike to show, also under these conditions, the different time course of the return to the initial resting membrane potential of −50 mV. *C*, I_{AHP} summation during trains of 20 Hz voltage pulses of constant duration (6 ms) but of increasing amplitude (*a*, −50 to −20; *b*, −50 to −10; *c*, −50 to 0 mV). The calculated amount of Ca^{2+} charge injected by each voltage step was 9, 26 and 50 pC, respectively. *D*, I_{AHP} summation during trains of 5 ms constant voltage steps to −20 mV applied at increasing frequencies (5, 10, 15 and 20 Hz). Holding potential was −50 mV.

I_{AHP} peak amplitude evoked by the first pulse increased, as expected, with increasing pulse amplitude and, therefore, Ca^{2+} load (9, 26 and 50 pC are the calculated Ca^{2+} charges injected by each pulse in the three different trains). Correspondingly, the steady-state I_{AHP} saturation level increased and a new decay rate, depending on the final I_{AHP} amplitude, was observed. In Fig. 4*D*, constant −50 to −20 mV steps of 5 ms duration were applied in successive trains at different frequencies (5, 10, 15 and 20 Hz). Summation of the I_{AHP} was present at various degrees with the different frequencies tested and the steady-state level increased with increasing stimulation rate. I_{AHP} build-up developed independently of the activation rate, while the final saturation level (and the decay rate at the end of Ca^{2+} injection) depended on both the width of the single depolarizing step and the frequency of its application. At the onset of the summation process, each successive I_{AHP} seemed to contribute a current change which was of a different amplitude from the current amplitude of the preceding I_{AHP}. This was observed in all neurones, a feature which would not be expected during the very first pulses if the AHP conductance increase represents the summation of constant amounts of g_{AHP}. In fact, when Ca^{2+} was applied through single depolarizing steps of increasing amplitude and duration, the relationship between g_{AHP} and Ca^{2+} load proved linear over a wide range of injected Ca^{2+}. This discrepancy, however, is based on the assumption that the amount of Ca^{2+} injected by each individual step is independent of the step number in the series. In the sympathetic neurone, I_{Ca} inactivation shows properties which can provide a partial explanation for this behaviour. A memory of previous inactivation (the inactivation removal time constant was 1·5 s at −50 mV; Belluzzi & Sacchi, 1989) produces some degree of summation, is responsible for a persistent depression of I_{Ca}, and is most probably the basis for the progressive shortening of the calcium spike during repetitive activation of the neurone under current-clamp conditions. This would suggest that the amount of Ca^{2+} actually injected by repeated pulses is not constant but, because of inactivation summation, it progressively diminishes as the number of steps in a train increases.

I_{AHP} influence on neuronal excitability

In the preceding section we have demonstrated that I_{AHP} summated when depolarizing steps were repeated sufficiently close to each other, even when they were as short as those associated with action potential development. The next step was to determine the practical effect of this summated outward current on neurone behaviour, tested within the membrane voltage range in which the I_{AHP} is expected to play a crucial role because of its voltage independence. This issue was examined under two different experimental conditions: (1) the response to isolated long-duration current pulses of different intensity, and (2) the response to just-threshold depolarizing steps applied at different rates in order to check for modifications in cell excitability.

In response to maintained depolarization, the discharge of sympathetic neurones adapted rapidly, typically after the first spike (less frequently after the second) when the cell fell silent throughout the duration of the pulse (for example, see Fig. 7*A*). Increasing the size of the depolarization or starting from larger holding potentials had no practical effect on this behaviour. I_{AHP} differs pharmacologically from other K^+ currents in the ganglion neurones. Previous experiments have shown that apamin and D-tubocurarine depress I_{AHP} in the bullfrog sympathetic neurone and in other systems (Nohmi & Kuba, 1984; Cook & Haylett, 1985; Bourque & Brown, 1987; Goh & Pennefather, 1987; Tanaka & Kuba, 1987) although for rat sympathetic neurones support for the involvement of a Ca^{2+}-activated K^+ conductance has been only indirectly obtained in current-clamp experiments (Kawai & Watanabe, 1986). This latter result was confirmed in the present voltage-clamp experiments in which 100 nM apamin significantly depressed I_{AHP} development (a mean of 86% in 4 cells). Virtually complete block of this current was achieved with 0·2–0·5 mM D-tubocurarine, which abolished not only the I_{AHP} following a single depolarizing step but also the summation of any residual I_{AHP} during a 20 Hz train of −50 to −20 mV steps of 5 ms duration (Fig. 5*A*). The expected AHP build-up under current-clamp conditions during a series of action potentials elicited by direct stimulation of the neurone was similarly blocked (Fig. 5*B*). D-Tubocurarine was thus regarded as a virtually specific and full blocker of I_{AHP}. Apamin or curare markedly attenuated the spike frequency adaptation so that one can be reasonably certain that the two responses represent the same phenomenon. If a long depolarizing current pulse was applied under the new conditions, in fact, the neurone could be made to fire during the time when it normally would have been silent. The input–output relationship of individual neurones could thus be determined by injecting 400–600 ms depolarizing current pulses of varying amplitude and plotting the steady-state firing against the current amplitude (*f–I* curve). The number of spikes evoked increased with injected current magnitude; the new firing rate was maintained at a fairly constant level when depolarization was mild (Fig. 5*C*), but only for a short time when the strong, sustained membrane depolarization caused I_{Na} inactivation. At least eight to ten full-size action potentials were usually elicited before the cell was unable to produce further spikes, hence its *f–I* relationship was observed over a reasonably wide range of current injections (Fig. 6*A*). In all neurones examined in the presence of D-tubocurarine, firing frequency increased in a nearly linear fashion with the level of injected current; the slope of the *f–I* relationship was 32·5 spikes nA^{-1} in the cell illustrated in Fig. 6*A*, with a mean value of 26·2 spikes nA^{-1} in our sample of eight cells. The neurone shown in Fig. 6*A* (open circles) was held at −50 mV; in the same cell the frequency *versus* current plot was duplicated by applying the same series of square current pulses starting from larger holding potentials (−60 to −90 mV voltage

range). The results obtained from the −80 mV trials are illustrated in Fig. 6*A* (filled circles). The average neuronal excitability was reduced but the slope of the *f–I* relationship remained the same as that for the −50 mV series (31·8 *vs.* 32·5; not statistically different according to Student's *t* test). A rightward shift of the straight line fitting the experimental points was noticed which, however, proved to correspond to the holding current required to move the membrane potential from −50 mV to the new imposed level. A possible role of I_A in repetitive firing, additional or complementary to I_{AHP}, might have been detected following removal of its −50 mV inactivation at more negative potentials (Belluzzi *et al.* 1985; Belluzzi & Sacchi, 1991). The data presented in Fig. 6*A*, however, suggest that I_A did not contribute significantly to tonic neuronal activity, at least not under the present experimental conditions in which maintained depolarization moved membrane fluctuations towards a voltage range at which I_A channels are permanently inactivated.

These results indicate a clear-cut role of I_{AHP} in neuronal accommodation which is strong enough, when operating, to damp any repetitive activity of the cell during maintained depolarization. The natural mode of activation of the sympathetic neurone, however, is not via long-duration current inflow but, on the contrary, by application of short-lived pulses impinging at random onto the cell through the presynaptic fibres (Blackman, 1974; Polosa *et al.* 1979). A more physiological test was thus undertaken, in which different spike rates were simulated by injecting trains of brief current pulses (2–3 ms) at frequencies between 1 and 20 Hz. Current pulses were sufficiently short to avoid

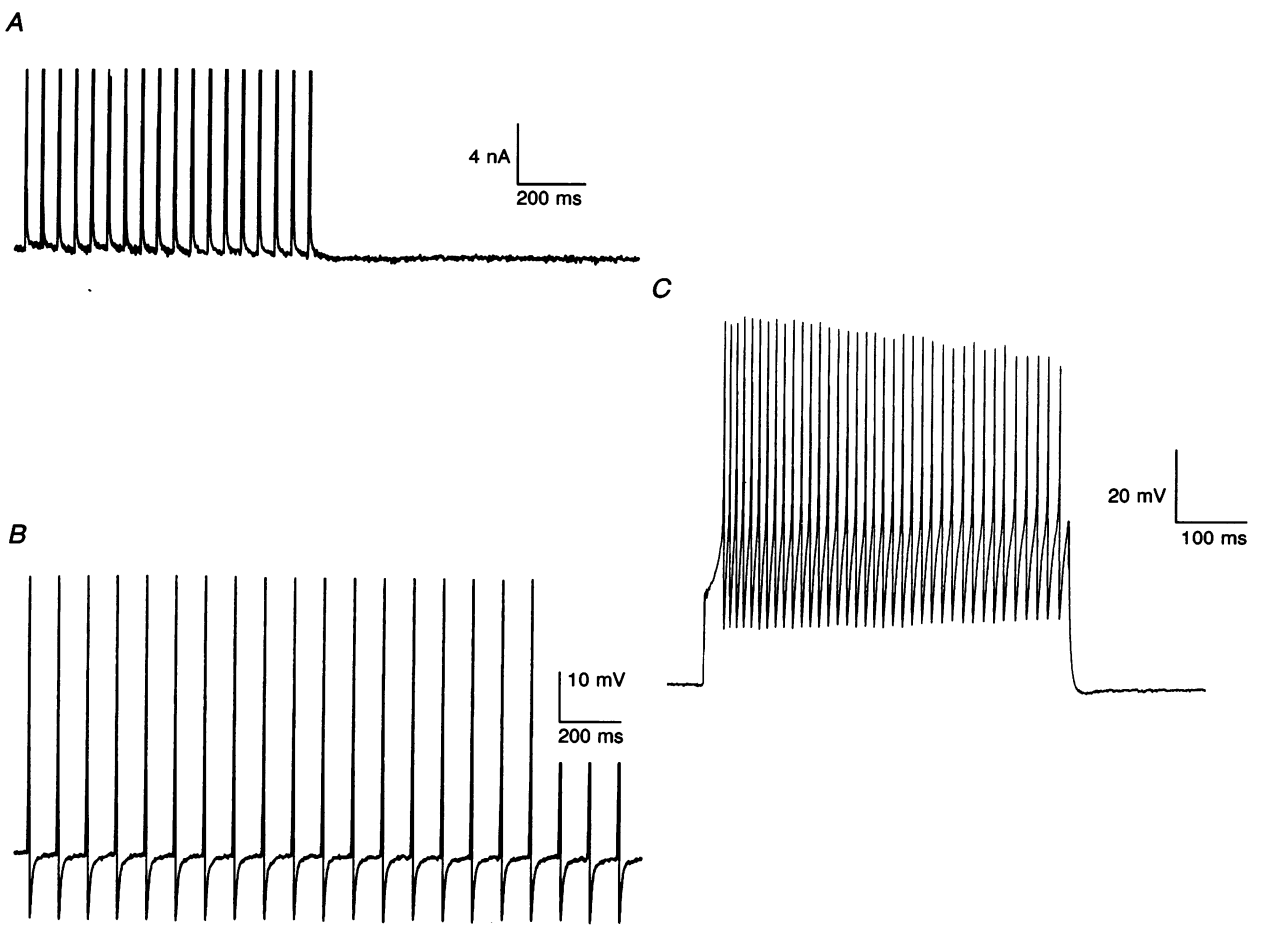

Figure 5. Blockade of the I_{AHP} by D-tubocurarine

A, a train of −50 to −20 mV voltage-clamp steps of 5 ms duration was applied to the same neurone shown in Fig. 4*D*, about 5 min after exposure to 0·25 mM D-tubocurarine. *B*, the train of action potentials (truncated) evoked at 10 Hz under two-electrode current-clamp conditions by brief depolarizing current pulses applied through the current electrode to show the absence of any AHP summation. Only the fast spike hyperpolarization sustained by the unaffected $I_{K,Ca}$ persisted, but $I_{K,Ca}$ turn-off kinetics during the interspike period at the −50 mV holding potential were too fast to allow any current summation. *C*, repetitive firing was evoked by a long-lasting depolarizing current pulse only after blockade of the I_{AHP} by exposure to 0·25 mM D-tubocurarine. The neurone was maintained at an initial holding potential of −80 mV.

prolongation of the normal, spike-activated Ca^{2+} influx and their strength was initially set just above that required to elicit a single, isolated action potential. At 1 Hz, depolarizing pulses consistently induced action potentials; however, as frequencies increased, the number of stimuli that resulted in failure grew to a point where the neurone became permanently silent and the threshold current had to be increased to allow the cell to begin firing action potentials again. This effect was consistent, as illustrated in Fig. 6*B* for a sample of eight neurones tested at the holding potential of −50 mV, since the threshold depolarizing charge increased by a factor of 1·4 at 5 Hz, 1·8 at 10 Hz and 2·5 at 20 Hz. This result was qualitatively independent of holding potential, as illustrated in the same neurone for the −40 to −60 mV voltage range (Fig. 6*C*). The low-rate threshold charge increased with an increase in the initial voltage level, as expected in the presence of a larger holding current and following partial removal of I_A inactivation at −60 mV. The requirement for progressively larger stimuli with higher stimulation rates was apparent at the three holding levels that could be tested in this neurone. The occurrence of action potentials was accompanied by a progressive hyperpolarization of the membrane, suggesting that a hyperpolarizing conductance was accumulating during repetitive stimulation. The hyperpolarization was not stable between successive spikes, repeating the membrane potential trajectory observed during isolated spikes at a more negative level; in the −50 mV experiments its mean value, measured at the foot of the spike, was 3·1, 7·0 and 9·9 mV during the 5, 10 and 20 Hz trains, respectively. Both these effects, namely the increase in threshold depolarizing charge and interspike hyperpolarization, were abolished by D-tubocurarine (Fig. 6*B*, open circles) or apamin; under these conditions the overall excitability of the cell was unaffected and spike trains could be elicited by constant intensity pulses over the whole 1–20 Hz frequency range.

I_{AHP} model and simulations

Recorded I_{AHP} tracings were described assuming that the mechanism underlying the slow conductance change involves simply activation and inactivation, and that both processes are voltage independent. The current was considered to rise exponentially to a maximum value; simultaneously, the current was also assumed to inactivate with a much slower exponential process. It was modelled as a difference between two exponentials according to the following equation:

$$I_{AHP} = \bar{g}_{AHP}(V - E_K)\{[\exp-(t/\tau_1)] - [\exp-(t/\tau_2)]\}, \quad (1)$$

where τ_1 is the time constant of the decay phase as

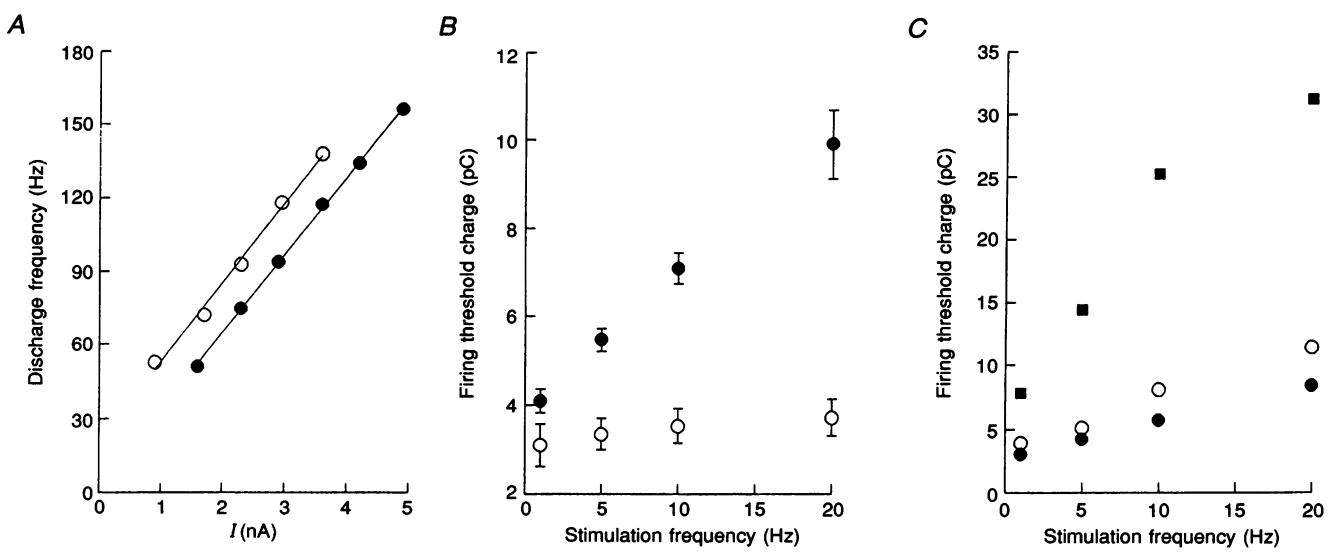

Figure 6. I_{AHP} contribution during repetitive firing

A, relationship between firing rate (averaged over the 58–550 ms firing periods during repeated 600 ms depolarizing current steps) and applied current intensity (*f–I* curve) in a sympathetic neurone exposed to 0·25 mM D-tubocurarine. The neurone was held at −50 mV (○) and then at −80 mV (●) membrane potential. The slopes of the regression lines through data points are not appreciably different. *B*, amount of depolarizing charge required to maintain a steady-state spike discharge in a sympathetic neurone directly stimulated by 3 ms current pulses at different frequencies in control solution (●, mean data from 8 neurones, V_h at −50 mV) and 5–8 min after exposure to 0·5 mM D-tubocurarine (○, data from 5 neurones, V_h at −50 mV). Bars represent the S.E.M. *C*, threshold charge for steady-state firing at different frequencies in a neurone maintained in control solution at different holding levels (−40 mV, ●; −50 mV, ○; −60 mV, ■). Spikes were evoked by repeated 3 ms current pulses applied through the current electrode.

determined directly from the decay of the slow tail current, and τ_2 is the onset time constant; both were considered virtually voltage independent over the voltage range tested. For the present calculations, τ_2 values could be obtained with some precision only for cells in which a clear peak of I_{AHP}, separated from the large fast component decay, could be recognized, as in the example shown in Fig. 3*E*. This behaviour is common for some mammalian neurones such as the rat CA1 pyramidal cells (Lancaster & Adams, 1986) and the guinea-pig myenteric and vagal neurones (Hirst *et al.* 1985; Sah & McLachlan, 1991), but was only occasionally observed in rat sympathetic neurones in which the fast voltage-dependent $I_{K,Ca}$ plus I_{KV} components continued smoothly into the slow I_{AHP} tail current. Least squares regression fitting of eqn (1) to the tracings provided imprecise τ_2 estimates, so we decided to assume that the I_{AHP} onset time constant was of the same size as the $I_{K,Ca}$ and I_{KV} decay time constants (5 ms). A short rise time constant means that a significant amount of I_{AHP} was activated by the spike itself, and this was a common experience with normal neurones. Moreover, maximum current activation of single SK channels in rat hippocampal neurones in culture was observed within 30 ms following fast exposure of excised patches to 1 μM Ca^{2+} at room temperature (Lancaster *et al.* 1991), suggesting fast activation kinetics. Despite the incomplete experimental definition of the I_{AHP} turn-on process, the direct contribution by I_{AHP} to the overall neurone behaviour could be detected. Figure 3*F* shows how the model, including g_{AHP}, simulated under voltage-clamp conditions the fast and slow tail currents evoked in a neurone depolarized to 0 mV for 5 ms and then returned to −50 mV holding potential (the same protocol as in Fig. 3*E*). The simulation was repeated in the absence of the total Ca^{2+}-dependent current fraction, to show the I_{KV} component in isolation.

When simulating the neuronal properties under current-clamp conditions in response to a long-lasting depolarizing current, the computation of membrane voltage and magnitude of the underlying currents proceeded in the following sequence. As previously suggested, the amount of g_{AHP} activated by an isolated action potential in the rat sympathetic neurone was taken as 10 nS; this is the value for g_{AHP} in eqn (1), which started operating when the Ca^{2+} charge injected into the neurone by the first spike was larger than a threshold value of 5 pC. The ensuing I_{AHP} was governed by the driving force for K^+ ions, the voltage-independent onset time constant of 5 ms and the decay rate, which was readily determined from the equation relating τ_1 and g_{AHP} (the straight line in Fig. 2*C*). If a second action potential was generated by the stimulating current, the new amount of Ca^{2+} entering the cell during the second spike was calculated. This value was summated to the initial 11 pC of Ca^{2+} charge related to the first spike,

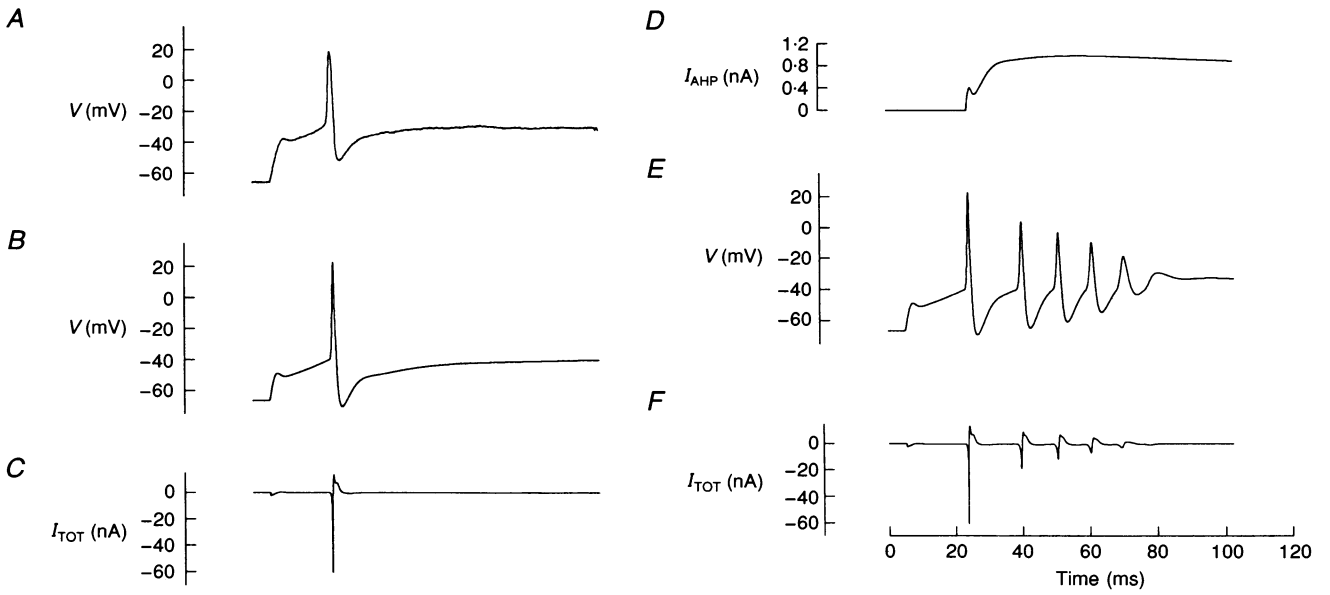

Figure 7. Role of I_{AHP} in regulating neuronal excitability

A, a single spike is evoked during application of a 2·4 nA depolarizing current pulse of 160 ms duration. Resting membrane potential was −66 mV. *B–D*, simulations from the six-conductance model of the rat sympathetic neurone (I_{Na}, I_{Ca}, I_A, $I_{K,Ca}$, I_{KV} and I_{AHP}) following injection of the same current pulse as in *A*. The current-clamp response is shown in *B*. In *C* the total (active plus passive components) transmembrane current underlying the tracing in *B* is represented with the I_{AHP} current time course separately illustrated in *D*. *E*, the g_{AHP} is removed from the model, otherwise set as in *B*; the ideal neurone now exhibits a clear-cut tendency to repetitive firing. The total current generating the tracing in *E* is shown in *F*. The time scale in *F* applies to all tracings.

giving a larger amount of total Ca^{2+} injected, which was expected to generate a larger I_{AHP} (according to the equation relating Ca^{2+} load and g_{AHP} activation; the straight line in Fig. 2*A*) and a new τ_1 value for current decay.

The results of some simulations are illustrated in Fig. 7. In Fig. 7*A*, in a real cell the depolarizing current evoked a single spike. In Fig. 7*B*, the simulated behaviour of an ideal neurone (with the same resistance–capacitance properties as the real neurone) is shown under current-clamp conditions following application of the same stimulating current. The total transmembrane current was calculated and is depicted in Fig. 7*C*, while Fig. 7*D* shows the underlying I_{AHP} time course in isolation. The behaviour of the same neurone when the I_{AHP} component was abolished is illustrated in Fig. 7*E* (with the corresponding currents in panel *F*) to demonstrate the new tendency to repetitive firing.

DISCUSSION

The present study examined some properties of isolated or summated I_{AHP} of rat sympathetic neurones. An empirical relationship was found between activated g_{AHP} and both the amount of Ca^{2+} load during activity and the g_{AHP} time course. Only a small fraction (about 15%) of the g_{AHP} maximum activation observed in the present experiments was attained during a single spike which was, however, sufficient to exert a braking action on spike discharge. Agents such as apamin or D-tubocurarine, which selectively block I_{AHP}, induced repetitive firing in a neurone which usually responded to prolonged depolarization with a single action potential. We demonstrated that g_{AHP} summated with repeated voltage pulses applied within tenths of milliseconds of each other. Our results suggest that a g_{AHP}-mediated mechanism was not only operative after firing but also during the course of stimulation at physiological frequencies, thus adjusting cell excitability to the spiking rate.

In the present study the Ca^{2+} dependence of I_{AHP} was shown most clearly by its relationship to the calcium current. When I_{Ca} was increased either by increasing the level of depolarization or by lengthening the period of Ca^{2+} entry, there was a corresponding increase in the maximum slow outward current. To a great extent the activated g_{AHP} and the amount of injected Ca^{2+} were linearly related with a ratio of 0·3 nS pC^{-1}. We were unable to assess whether a delay existed between the onset of I_{Ca} and the priming of I_{AHP} which, in any case, required a much larger Ca^{2+} inflow to reach threshold than did $I_{K,Ca}$ (7 *vs.* 0·15 pC). These differences might be related to the spatial distribution of intracellular Ca^{2+} after excitation and the location and densities of the different types of channels. Simultaneous patch-clamp and fura-2 microfluorimetric recordings of I_{Ca} and the intracellular free Ca^{2+} concentration in neurones from rat dorsal root ganglia have demonstrated a linear relationship, before saturation, between the peak of $[Ca]_i$ transients and the integrated I_{Ca} over a wide range of Ca^{2+} loads (Thayer & Miller, 1990). Using confocal fluorescence microscopy, calcium concentrations as high as 0·6 μM were detected in the periphery of dissociated bullfrog sympathetic neurones following voltage-clamp pulses to +10 mV of 100 ms duration; prior to redistribution through the cytoplasm, such Ca^{2+} levels are sufficiently high to sustain activation of the I_{AHP} (Hernández-Cruz, Sala & Adams, 1990). These findings, together with the slow dissipation of Ca^{2+} gradients, are consistent with the I_{AHP} properties and make tenable the suggestion that the I_{AHP} intensity and time course are to some extent related to the rate of $[Ca]_i$ removal and buffering near its point of entry.

In the sympathetic neurone, g_{AHP} accounted for only a minor fraction (7%) of the total Ca^{2+}-activated conductance (some 18% in GH3 cells; Lang & Ritchie, 1987). The peculiar characteristics of I_{AHP}, as in other neurones, were its voltage independence and high Ca^{2+} sensitivity, even at negative membrane potentials, thus justifying its presence as a unique current at voltage levels which rapidly close any other voltage-dependent channels. SK channels have been described in a variety of excitable cells and apparently share many properties with I_{AHP}, to the point that they are likely candidates for maintaining the resting membrane potential of the neurone. We found, however, that barium substitution for calcium, calcium antagonists such as Cd^{2+}, exposure to D-tubocurarine and similar treatments preventing the occurrence of the slow I_{AHP} had no effect on the passive properties of the sympathetic neurone at membrane voltages negative to −40 mV (O. Sacchi, unpublished observations). This would suggest that the very sensitive g_{AHP} mechanism (the open probability of SK channels of rat pituitary cells and hippocampal neurones at −50 mV is 0·5 at an external Ca^{2+} concentration of 1 μM, but 0 at 500 nM; Lang & Ritchie, 1987; Lancaster *et al.* 1991) is actually a minor factor in determining the resting conductance of the sympathetic neurone. The SK channels remain open as long as a gradient of $[Ca^{2+}]_i$ is present (without inactivation or desensitization even with very long Ca^{2+} application; Lancaster *et al.* 1991) but they are unable to detect very low intracellular resting Ca^{2+} concentrations.

We have no direct measure of the saturation conductance of I_{AHP}, but conductances as high as 70 nS have repeatedly been measured in the present experiments. Single-channel conductance values for Ca^{2+}-activated SK channels are in the range of 5–15 pS (Blatz & Magleby, 1986; Lang & Ritchie, 1987; Lancaster *et al.* 1991; Leinders & Vijverberg, 1992; Artalejo *et al.* 1993), but a unitary SK conductance of 3–5 pS is most probably a more appropriate estimate under a physiological K^+ gradient (Lang & Ritchie, 1987; Leinders & Vijverberg, 1992; Artalejo *et al.* 1993). If the channels responsible for I_{AHP} in the rat sympathetic neurone are within the above range of conductances, then a minimum of 18000 SK channels (a mean of 8–9 channels

per square micrometre of somatic membrane) are likely to be opened during maximal I_{AHP} activation and some 2000–2500 channels at the peak of the spike after-hyperpolarization.

The results shown in Fig. 6*B* would indicate that a tight interaction exists between the threshold charge for firing and the firing frequency. The practical result is that an excitatory input which is suprathreshold for the neurone at a low activation rate becomes inadequate to fire the cell when applied at higher frequencies or, in other words, a very different top discharge frequency exists for any excitatory event of constant strength repeated at variable frequencies. The g_{AHP}, which is silent under resting conditions, contributed to membrane conductance at potentials near rest as long as the cytosolic Ca^{2+} concentration remains elevated. Ca^{2+} entering the neurone during repetitive activity accumulates and maintains a background membrane conductance which, at 20 Hz, is comparable to that observed at the peak of the AHP during an isolated action potential. From the initial resting level of −50 mV, the 10 mV hyperpolarization measured at the foot of the action potential was expected to increase the spiking threshold charge in the cell model by nearly 45% (20% in the case of the 7 mV hyperpolarization during the 10 Hz train). These figures are much lower than those observed in the experiments, in which the threshold charge actually increased by 250 and 180% for the 20 and 10 Hz activation rate, respectively. A stable opposing conductance is thus expected to accumulate during the train as a consequence of a steady-state activation of the g_{AHP} machinery.

An additional comment is needed on the role of the holding membrane potential. Figure 6*C* shows, for example, that an isolated excitatory charge just suprathreshold to maintain a 1 Hz firing rate at a membrane potential of −60 mV became adequate to sustain a 20 Hz discharge rate in the same neurone held at −40 mV. Simulations and experimental data confirm the dominant role of a persistent g_{AHP} also under these circumstances, since this behaviour was insufficiently explained in our model on the basis of simple voltage-related modifications of the kinetic parameters of the various currents present in the cell.

The activation rates used in the present experiments are well within the range of the discharge frequencies observed in pre- and postganglionic sympathetic fibres (Polosa *et al.* 1979; Skok & Ivanov, 1987; Ivanov & Purves, 1989). Frequency and intensity of ongoing synaptic activity, actual membrane potential level and g_{AHP} activation thus represent a complex mix of mutually related factors controlling the final firing rate of the sympathetic neurone in the normally operating nervous network and ultimately its ability to encode information. The small g_{AHP} system participates in the intrinsic feedback loop through which the Ca^{2+} inflow sustained by action potential activity generates increasing membrane hyperpolarization, thus adjusting with every spike cell excitability.

Artalejo, A. R., García, A. G. & Neher, E. (1993). Small-conductance Ca^{2+}-activated K^+ channels in bovine chromaffin cells. *Pflügers Archiv* **423**, 97–103.

Belluzzi, O. & Sacchi, O. (1989). Calcium currents in the normal adult rat sympathetic neurone. *Journal of Physiology* **412**, 493–512.

Belluzzi, O. & Sacchi, O. (1990). The calcium-dependent potassium conductance in rat sympathetic neurones. *Journal of Physiology* **422**, 561–583.

Belluzzi, O. & Sacchi, O. (1991). A five-conductance model of the action potential in the rat sympathetic neurone. *Progress in Biophysics and Molecular Biology* **55**, 1–30.

Belluzzi, O., Sacchi, O. & Wanke, E. (1985). A fast transient outward current in the rat sympathetic neurone studied under voltage-clamp conditions. *Journal of Physiology* **358**, 91–108.

Blackman, J. G. (1974). Function of autonomic ganglia. In *The Peripheral Nervous System*, ed. Hubbard, J. I., pp. 257–276. Plenum Press, New York.

Blatz, A. L. & Magleby, K. L. (1986). Single apamin-blocked Ca-activated K^+ channels of small conductance in cultured rat skeletal muscle. *Nature* **323**, 718–720.

Bourque, C. W. & Brown, D. A. (1987). Apamin and D-tubocurarine block the afterhyperpolarization of rat supraoptic neurosecretory neurons. *Neuroscience Letters* **82**, 185–190.

Cook, N. S. & Haylett, D. G. (1985). Effects of apamin, quinine and neuromuscular blockers on calcium-activated potassium channels in guinea-pig hepatocytes. *Journal of Physiology* **358**, 373–394.

Ginsborg, B. L. (1973). Electrical changes in the membrane in junctional transmission. *Biochimica et Biophysica Acta* **300**, 289–317.

Goh, J. W. & Pennefather, P. S. (1987). Pharmacological and physiological properties of the after-hyperpolarization current of bullfrog ganglion neurones. *Journal of Physiology* **394**, 315–330.

Hernández-Cruz, A., Sala, F. & Adams, P. R. (1990). Subcellular calcium transients visualized by confocal microscopy in a voltage-clamped vertebrate neuron. *Science* **247**, 858–862.

Hirst, G. D. S., Johnson, S. M. & van Helden, D. F. (1985). The slow calcium-dependent potassium current in a myenteric neurone of the guinea-pig ileum. *Journal of Physiology* **361**, 315–337.

Ivanov, A. & Purves, D. (1989). Ongoing electrical activity of superior cervical ganglion cells in mammals of different size. *Journal of Comparative Neurology* **284**, 398–404.

Kawai, T. & Watanabe, M. (1986). Blockade of Ca-activated K conductance by apamin in rat sympathetic neurones. *British Journal of Pharmacology* **87**, 225–232.

Lancaster, B. & Adams, P. R. (1986). Calcium-dependent current generating the afterhyperpolarization of hippocampal neurons. *Journal of Neurophysiology* **55**, 1268–1282.

Lancaster, B., Nicoll, R. A. & Perkel, D. J. (1991). Calcium activates two types of potassium channels in rat hippocampal neurons in culture. *Journal of Neuroscience* **11**, 23–30.

Lang, D. G. & Ritchie, A. K. (1987). Large and small conductance calcium-activated potassium channels in the GH3 anterior pituitary cell line. *Pflügers Archiv* **410**, 614–622.

Latorre, R., Oberhauser, A., Labarca, P. & Alvarez, O. (1989). Varieties of calcium-activated potassium channels. *Annual Review of Physiology* **51**, 385–399.

LEINDERS, T. & VIJVERBERG, H. P. M. (1992). Ca^{2+} dependence of small Ca^{2+}-activated K^+ channels in cultured N1E-115 mouse neuroblastoma cells. *Pflügers Archiv* **422**, 223–232.

MCAFEE, D. A. & YAROWSKY, P. J. (1979). Calcium-dependent potentials in the mammalian sympathetic neurone. *Journal of Physiology* **290**, 507–523.

MARTY, A. (1981). Ca-dependent K channels with large unitary conductance in chromaffin cell membranes. *Nature* **291**, 497–500.

MORITA, K. & KATAYAMA, Y. (1989). Calcium-dependent slow outward current in visceral primary afferent neurones of the rabbit. *Pflügers Archiv* **414**, 171–177.

NOHMI, M. & KUBA, K. (1984). (+)-Tubocurarine blocks the Ca^{2+}-dependent K^+-channel of the bullfrog sympathetic ganglion cells. *Brain Research* **301**, 146–148.

PENNEFATHER, P., LANCASTER, B., ADAMS, P. R. & NICOLL, R. A. (1985). Two distinct Ca-dependent K currents in bullfrog sympathetic ganglion cells. *Proceedings of the National Academy of Sciences of the USA* **82**, 3040–3044.

POLOSA, C., MANNARD, A. & LASKEY, W. (1979). Tonic activity of the autonomic nervous system: functions, properties, origins. In *Integrative Functions of the Autonomic Nervous System*, ed. BROOKS, C. MCC., KOIZUMI, K. & SATO, A., pp. 342–354. University of Tokyo Press, Tokyo.

SAH, P. & MCLACHLAN, E. M. (1991). Ca^{2+}-activated K^+ currents underlying the afterhyperpolarization in guinea pig vagal neurons: a role for Ca^{2+}-activated Ca^{2+} release. *Neuron* **7**, 257–264.

SKOK, V. I. & IVANOV, A. Y. (1987). Organization of presynaptic input to neurones of a sympathetic ganglion. In *Organization of the Autonomic Nervous System: Central and Peripheral Mechanisms*, ed. CIRIELLO, J., CALARESU, F. R., RENAUD, L. P. & POLOSA, C., pp. 37–46. Alan Liss, New York.

SMART, T. G. (1987). Single calcium-activated potassium channels recorded from cultured rat sympathetic neurones. *Journal of Physiology* **389**, 337–360.

TANAKA, K. & KUBA, K. (1987). The Ca^{2+}-sensitive K^+-currents underlying the slow afterhyperpolarization of bullfrog sympathetic neurones. *Pflügers Archiv* **410**, 234–242.

THAYER, S. A. & MILLER, R. J. (1990). Regulation of the intracellular free calcium concentration in single rat dorsal root ganglion neurones *in vitro*. *Journal of Physiology* **425**, 85–115.

Acknowledgements

We thank Professor A. Nistri for many helpful comments on the manuscript. This paper has been supported by grants from the Ministero della Università e della Ricerca Scientifica e Tecnologica, and from the Italian Consiglio Nazionale delle Ricerche.

Received 1 February 1994; accepted 28 July 1994.